ELSEVIER

Spectrochimica Acta Part B 60 (2005) 1025 – 1033

SPECTROCHIMICA ACTA PART B

www.elsevier.com/locate/sab

Filament-induced remote surface ablation for long range laser-induced breakdown spectroscopy operation☆

Ph. Rohwetter[a], K. Stelmaszczyk[a], L. Wöste[a], R. Ackermann[b], G. Méjean[b], E. Salmon[b], J. Kasparian[b], J. Yu[b,*], J.-P. Wolf[b]

[a]*Fachbereich Physik der Freien Universität Berlin, Institut für Experimentalphysik, Arnimallee 14, D-14195 Berlin, Germany*
[b]*Laboratoire de Spectrométrie Ionique et Moléculaire (LASIM), UMR CNRS 5579, Université Claude Bernard-Lyon 1, 43, Bd. du 11 Novembre 1918, F-69622 Villeurbanne Cedex, France*

Received 13 December 2004; accepted 22 March 2005
Available online 16 June 2005

Abstract

We demonstrate laser induced ablation and plasma line emission from a metallic target at distances up to 180 m from the laser, using filaments (self-guided propagation structures ~100 μm in diameter and $\sim 5 \times 10^{13}$ W/cm^2 in intensity) appearing as femtosecond and terawatt laser pulses propagating in air. The remarkable property of filaments to propagate over a long distance independently of the diffraction limit opens the frontier to long range operation of the laser-induced breakdown spectroscopy technique. We call this special configuration of remote laser-induced breakdown spectroscopy "remote filament-induced breakdown spectroscopy". Our results show main features of filament-induced ablation on the surface of a metallic sample and associated plasma emission. Our experimental data allow us to estimate requirements for the detection system needed for kilometer-range remote filament-induced breakdown spectroscopy experiment.

Keywords: Laser filaments; Remote laser-induced surface ablation; Remote laser-induced breakdown spectroscopy

1. Introduction

Laser-induced breakdown spectroscopy (LIBS) is a laser-based versatile elemental analysis tool which attracts increasing attention today because of broad range of applications [1,2]. The increasing interest in the LIBS techniques is certainly due to their inherent features: atmospheric pressure all-optical excitation and detection, no need for sample preparation, multi-element analytical capability [1–3]. The recent progresses in the fundamentals of the LIBS technique, such as dual-pulse configuration [4] or femtosecond LIBS (Femto-LIBS) [5], and the introduction into the market of new types of spectrometers (multi-spectrometers [6], or échelle spectrometers [7]), do contribute to the evolution of the LIBS technique toward a more powerful analytical tool, allowing quantitative analysis or complex sample analysis including organic and biological samples [2].

The possibility of remote operation of LIBS is one of the properties which enlarge field of applications of this technique. Remote operation is required when samples to be analysed are difficult to access or located in hazardous areas. Examples would be minerals in a geological site, a chemically or nuclearly polluted industrial or urban site, or simply an edifice with polluted surface. Classical approach using a nanosecond pulsed laser for excitation is limited in range of operation by difficulty to tightly focus exciting laser beam at long distances. Obeying the laws of classical optics, diameter of focus linearly increases with focusing distance as a consequence of the

☆ This paper was presented at the 3rd International Conference on Laser Induced Plasma Spectroscopy and Applications (LIBS 2004), held in Torremolinos (Málaga, Spain), 28 September – 1 October 2004, and is published in the special issue of *Spectrochimica Acta Part B*, dedicated to that conference.

* Corresponding author.
E-mail address: jin.yu@lasim.univ-lyon1.fr (J. Yu).

0584-8547/$ - see front matter © 2005 Elsevier B.V. All rights reserved.
doi:10.1016/j.sab.2005.03.017

diffraction. Remote LIBS measurements performed at distances up to 120 m using nanosecond pulses have been reported by the group of Prof. Laserna in Malaga [8]. However, further increase of operation distance would require exorbitant large laser energy and large focusing optics which would become prohibitive for practical uses. Therefore carrying high laser fluence beyond the limitation of the diffraction to generate strong sparks on a sample at a long distance is a key point for a remote chemical identification and furthermore a remote chemical analysis by LIBS.

In this paper we demonstrate a new approach for long distance remote operation of LIBS technique. This approach is based on use of filaments formed by ultrashort and ultra-intense laser pulses propagating in air. We call this configuration remote filament-induced breakdown spectroscopy (R-FIBS) [9]. Briefly, filaments appear as a result of a dynamic equilibrium between Kerr lens focusing and defocusing on laser-induced micro-plasma. More precisely, due to nonlinear part of the refractive index, a laser pulse with peak power larger than a critical power (several GW in air) undergoes self-focusing and tends to collapse after a certain distance of propagation [10]. However, self-focusing goes into competition with a defocusing effect due to a partial ionization of air once self-focused laser intensity becomes high enough. Experimental observation [11] and theoretical calculation [12] show that a dynamic equilibrium establishes at an intensity of $\sim 5 \times 10^{13}$ W/cm^2 and a free electron density of $\sim 10^{16}$ cm^{-3} in laser-induced plasma [13,14]. Such equilibrium leads to a self-guided channel, called filament, with a diameter on the order of 100 μm. A single filament carries typically 1 mJ of pulse energy. The length of filaments has been observed exceeding 100 m [15]. With an initial focusing and/or initial pulse chirp, starting point of filaments can be controlled [16]. Filaments have been observed propagating at a distance of few kilometers from the laser [17]. High intensity inside the core of a filament leads to ablation on a target. The subsequent plasma line emission can then be detected by a suitable detection system coupled to a telescope remotely collecting light emitted from the plasma.

In following sections we first describe our experimental setup. In Experimental results, we present characteristics of the surface of a copper sample ablated by filaments together with the associated plasma emission spectra. The dependences of plasma line emission intensity as a function of an initial chirp of laser pulses are then presented for different distances between the laser and the sample. We show especially that for an increasing sample distance, R (up to 90 m limited by the available space in our experiments), it is always possible to optimize plasma emission with an adequate negative chirp. In such way, the plasma emission detected by a fixed detection system nearby the laser only decreases with the geometrical factor $1/R^2$. That means a constant plasma emission from the sample ablated by filaments independently on the sample distance. As an example of filament-induced ablation at long distance, we present the evidence of line emission from a plasma induced on an aluminum sample located at a distance of 180 m from the laser. In Section 4, we provide an estimation of requirements for the detection system to reach 1-km operation of LIBS using filaments.

2. Experimental setup

In our experiments, a container-integrated femtosecond terawatt laser system (Teramobile [18] system) was used. A detailed description of the laser system can be found elsewhere [16]. Briefly, a commercial chirped-pulse-amplification (CPA) [19] chain (Thales Laser Company) was integrated in a standard ISO container. The laser chain consisted of an oscillator, a stretcher, a regenerative amplifier, a preamplifier, a main amplifier and a compressor. Operating at a wavelength of 795 nm and a repetition rate of 10 Hz, the chain delivered pulses of up to 350 mJ energy and of 75 fs minimal duration.

The laser beam was sent towards the target collimated with a beam diameter of about 4.5 cm. An initial chirp was applied to laser pulses in order to initiate filaments at a defined distance to the sample. In order to have a precise control of chirp setting, one of the gratings in the compressor was mounted on a motorized linear translation. Initial pulse duration could be set from less than 100 fs to several picoseconds with either positive or negative chirps. Picosecond ($\sim$200 ps) or nanosecond ($\sim$5 ns) pulses at same energy per pulse as femtosecond pulses can also be generated from our system, by bypassing the compressor or by removing the injection from the oscillator, respectively.

A detection system was located beside the laser in the container. It consisted of a f/4 aperture Newtonian telescope with a primary mirror of 20 cm diameter. Light collected at the focus of the telescope was coupled into an optical fiber bundle. The output f-number of the fiber bundle was matched to the input of a f/8 (f=500 mm) spectrometer (Chromex 500IS/SM) equipped with a 1200 lines/mm diffraction grating. The detector of an ICCD camera (Princeton Instruments PI-MAX 1024HQ) was placed in the reciprocal plane of the spectrometer. The ICCD camera was triggered with a selectable delay with respect to the emission of a laser pulse. This detection system was used for the results presented in Sections 3.1, 3.2, and 3.3.

In a second detection system, a lens of 50 mm diameter and 250 mm focal focused plasma emission on the input end of a fiber. The fiber was directly connected to the input slit of a 250 mm focal length f/4 aperture grating spectrometer (Oriel MS257) equipped with a UV grating ruled with 600 lines/mm. At the output of the spectrometer, light was detected by a photomultiplier (PM) module (Hamamatsu

6780-03). This detection system could be placed near a sample to be able to locally detect plasma line emission. The result presented in Section 3.4 was obtained with this detection system.

3. Experimental results

3.1. Characteristics of filament-induced remote surface ablation on a metallic sample and associated plasma line emission

3.1.1. Remote surface ablation induced by filaments

As laser pulses were sent towards a sample in a parallel beam, ablation on the sample was induced by filaments only. With a pulse energy exceeding several tens of millijoules, multi-filamentation occurs, which denotes breaking up of the beam into a large number of self-guided substructures, carrying about 1 mJ energy in each filament. Multi-filamentation must be distinguished from collapse of a beam as a whole into one single filament. Filaments emerge from hot spots or generally from non-uniformities in the initial beam profile [20]. Fig. 1(a) shows a picture of a typical beam profile with many filaments (about 15 filaments) which appear as bright spots. Fig. 1(b) shows a picture of a copper sample irradiated by both a parallel laser beam containing filaments, and a focused laser beam for comparison. The black spot in the centre is due to a focused beam hitting the sample at a distance of 25 m from the laser. Other grey spots are caused by filaments contained in a parallel beam hitting the sample at a distance of 90 m from the laser. Spots due to filaments exhibit a diameter larger than filament diameter of about 100 μm, that is because of random walks around the mean position of a filament due to turbulent nature of filamentation process [20] and inhomogeneities in air. Such random walks lead to a superficial ablation of the sample even after a long time irradiation. Our previous works [16] (see also Section 3.2 below) show a dependence of the filament starting position on the initial pulse duration. To avoid a filamentation very close to the laser, which leads to weaker filaments at long distance, we applied a negative chirp on the pulse to increase its initial duration. The initial pulse duration for a filamentation at around 90 m is about 400 fs. When a filament starts, the laser pulse undergoes strong spectral and temporal modulations as shown by numerical simulations [21,22]. However, due to extreme high intensity inside of a filament, a direct measurement of pulse profile by the means of autocorrelation for example, is quite difficult.

We have inspected the surface of a copper sample irradiated by filaments with a scanning electron microscope (SEM). A corresponding SEM micrograph is shown in Fig. 2(a). For comparison, an SEM micrograph of a crater made by focused laser pulses is shown in Fig. 2(b). As one can see, the surface ablated by filaments exhibits a regular quasi-periodical ripple structure. The orientation of the ripples is perpendicular to the polarization of incident laser light. In our experiments, laser light was horizontally polarized. Observed ripples are then oriented in the vertical direction. Dominant spatial ripple is a sub-wavelength structure of period about 0.64 μm. In contrast, metal surfaces ablated by focused high-energy femtosecond laser pulses exhibit irregular microscopic structure due to higher fluence deposited on the sample in this configuration.

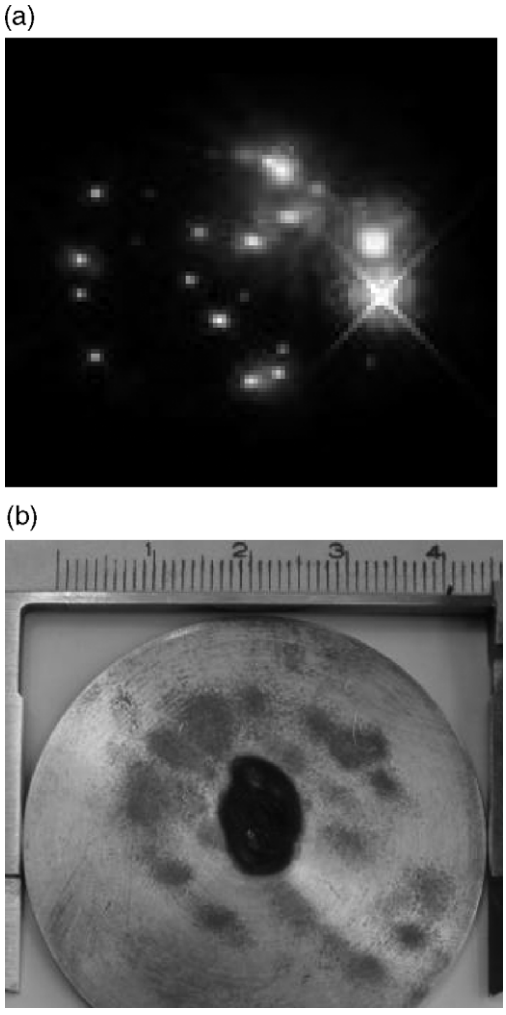

Fig. 1. (a) Picture of a typical laser beam profile with many filaments (single shot picture). On the picture, filaments appear as bright spots. Notice that each filament is surrounded by a conical emission in the visible range that increases the apparent size of the filaments on the picture to the order of mm. The whole beam had a diameter of 5 cm. (b) Picture of a copper sample irradiated by a large number of laser pulses. The black spot in the middle is due to irradiation with a focused beam from a distance of 25 m. Other grey spots are results of filament irradiation of the sample placed at a distance of 90 m. Random walks of a filament around its mean position due to inhomogeneities in air lead to a superficial ablation on a surface much larger than filament diameter. The scale of this picture is indicated by a ruler with a cm graduation in the upper part of the picture.

Similar ripple structures have been also reported for nanosecond pulse surface ablation [23]. According to the theory developed for long pulse duration laser irradiation [24], such patterns are due to interferences between incoming and anisotropically scattered light on surface

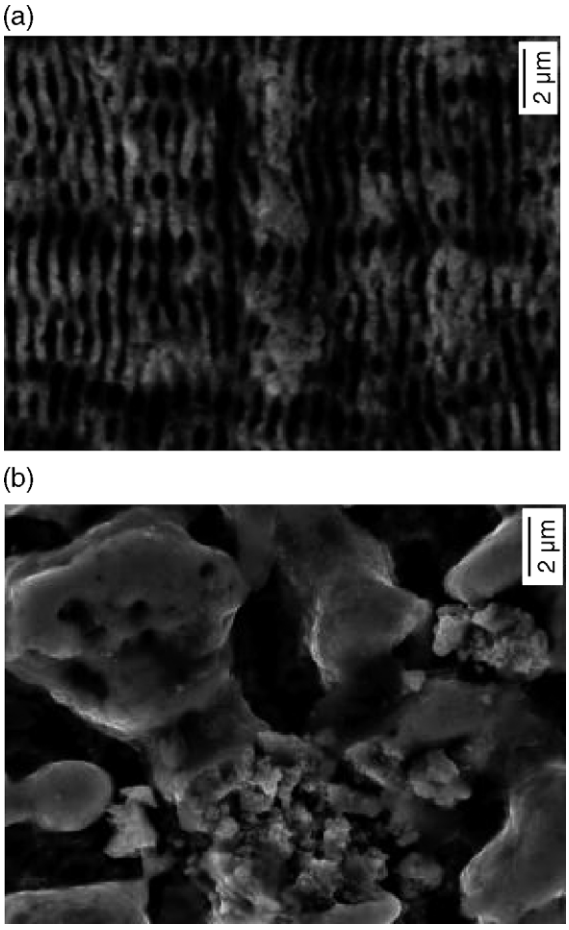

Fig. 2. SEM images of laser-ablated surface of a copper sample after a large number of laser pulse irradiation. (a) Irradiated by filaments, target at 90 from the laser, (b) irradiated by focused pulses, target at 25 m from the laser. A grating like ripple structure is clearly observed on the surface ablated by filaments. Ripples are oriented perpendicular to laser polarisation with a period of 0.64 μm. In contrast, focused pluses lead to a chaotic ablated surface at the microscopic scale.

roughness with sub-wavelength dimension. Such interferences result in inhomogeneous energy deposition on the surface. This process involves a feedback mechanism between evolving surface sub-wavelength structure and anisotropic energy deposition which leads to the observed steady-state surface pattern under certain threshold for laser fluence. This model predicts a sub-wavelength period for ripples when incident pulses are not in the normal direction with respect to the sample surface. Orthogonal direction of ripples with respect to laser polarization is also predicted by the model.

In ultra-short pulse regime, ripple structures have been recently reported for dielectric substrates such as BaF_2 or CaF_2 ablated by focused femtosecond pulses [25–27]. In this regime, the model based on interferences discussed above cannot be applied because of either short pulse duration or associated large pulse spectrum excluding any steady-state interference. The proposed model for ripple in ultra-fast regime is a self-organization from a chaotic state [25–27]. In this model, rapid excitation of electrons and surface ionization by the incident laser pulse induce a massive instability in the crystal lattice due to a perturbation of the interatomic bonds. The resulted instability characterized by positive charge accumulation and explosive emission of massive particles leads to a relaxation of the highly perturbed surface through surface reorganization by atomic diffusion. Such reorganization results mostly in regular and periodic structure. This model is supported by experimental observations [25–27] such as sensitivity to both wavelength and incident angle, observed ripple period significantly smaller than the incident wavelength, and bifurcations (also visible on our copper sample shown in Fig. 2(a)). Theoretical simulations of femtosecond ablation [28,29] support also the self-organization model. Our observation reported here provides the first evidence of surface ripples induced by femtosecond pulses on a metallic sample.

3.1.2. Filament-induced plasma emission spectra

Emission spectra of plasma induced by femtosecond laser pulses on metal samples in ambient air have been compared to those induced by picosecond or nanosecond pulses of same energy under the same atmospheric conditions. With femtosecond pulses, in focused geometry as well as in collimated ‘filament’ configuration, plasma line emission have been observed on a clean background, free from spectral emission of ambient air species. As shown in Fig. 3(a), in the spectral range between 700 nm and 900 nm, two atomic copper lines are observed without any background lines. In the same spectral range, with picosecond (or nanosecond) pulses additional non-copper lines are observed (Fig. 3(b)). These background lines represent atomic oxygen and atomic nitrogen emission. They are due to diffusive mixing of the expanding hot metal vapour with ambient gas [30] in the nanosecond pulse regime. In the picosecond pulse regime, emission from ambient gas is due to the interaction of the trailing part of the laser pulse with an early stage electron plasma leading to inverse bremsstrahlung heating of the plasm plume [31]. We interpret the absence of background lines in femtosecond pulse induced LIBS spectra as being a consequence of fundamental differences of laser-surface interaction in the different regimes of laser pulse duration. Especially, in the femtosecond regime, produced plasma plume is not enough energetic to excite ambient gas. A spectrum without background lines is highly appreciable for analysis and identification of complex biological samples such as bacteria [32]. Background lines overlapping with emission from sample can induce ambiguity in the analysis.

3.2. Optimizing filaments with a chirped pulse

3.2.1. Control of filament starting position by an initial negative chirp

Filament-induced plasma line emission intensity has been observed to depend critically on an initial chirp

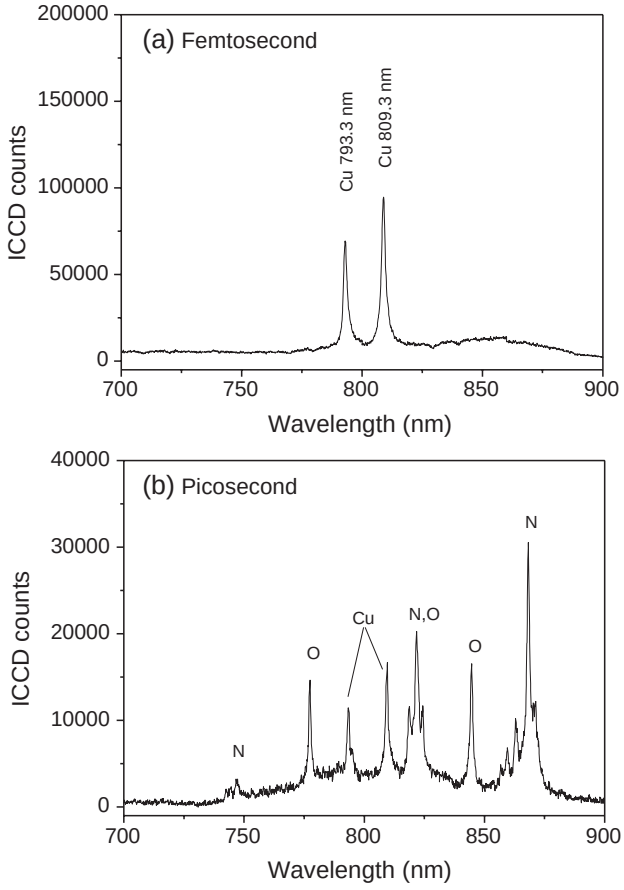

Fig. 3. Plasma line emission spectra from a copper sample excited by femtosecond pulses (a), and by picosecond pulses (b). With femtosecond pulses, two copper atomic lines in the spectral range from 700 nm to 900 nm are observed without any background lines. In contrast, with picosecond (or nanosecond pulses), the copper lines are mixed with background lines from ambient air: atomic oxygen (O) and atomic nitrogen (N) lines.

applied to laser pulses. That is because the starting position of filaments can be controlled by an initial chirp [16], and light intensity inside a filament varies as the filament propagates. Fig. 4 shows the result of an acoustic measurement on longitudinal profile of filaments induced by initially compressed 350 mJ femtosecond pulses. As we have shown elsewhere [33,34], measured acoustic signal is proportional to free electron density in the filaments. And via equilibrium between Kerr focusing and plasma defocusing, detected acoustic signal is finally related to light intensity in filaments.

From the result shown in Fig. 4, we can consider the development of filaments in three steps: onset of the filaments where the intensity increases, saturation of the filaments where the intensity reaches a maximum and remains constant, and finally damping of the filaments where the intensity decreases gradually. For initially compressed pulses, filaments build up quickly after travelling a short distance from the output of the laser, and reach the saturation at a distance of about 3.5 m from the window of the container. At a distance of about 12.5 the filament intensity starts to decrease. At a distance of about 40 m, free electron density falls down to a 10th of its maximal value.

In a remote LIBS experiment, for a certain distance between the laser and the sample, it is desirable to have the filaments hitting the target in their most intense phase. Imposing a negative chirp (“blue” first) on initial laser pulses is a suitable means for achieving a control of filamentation [16]. An initial negative chirp has in fact two effects: (1) it leads to a larger pulse duration and lower pulse peak power. This reduces initial Kerr-focusing and delays the onset of filamentation. (2) It pre-compensates the GVD of air. The negatively chirped pulse gets recompressed by the positive GVD of air, i.e. its peak power increases during propagation through air, in turn leading to increased Kerr focusing. The interplay of both effects allows prolonging the starting position of filaments to a long distance near the target.

3.2.2. Optimization of plasma line emission by an initial negative chirp

In Fig. 5, intensity of remotely detected line emission from filament-induced copper plasma is plotted versus initial duration of negatively chirped laser pulses for three different distances between the laser and the sample. We arbitrarily normalize the maximal intensities at different distances in order to focus attention on effects of the initial pulse duration due to a negative chirp for a given sample distance.

In Fig. 5, dashed parabolas do not represent theoretical fitting curves, but are intended to guide the eye. As can be seen in the figure, line emission intensity for different distance peaks at specific pulse durations corresponding to specific negative chirps. The larger the sample distance is, the longer is the initial pulse duration which optimizes plasma emission, that corresponds to the fact that a larger

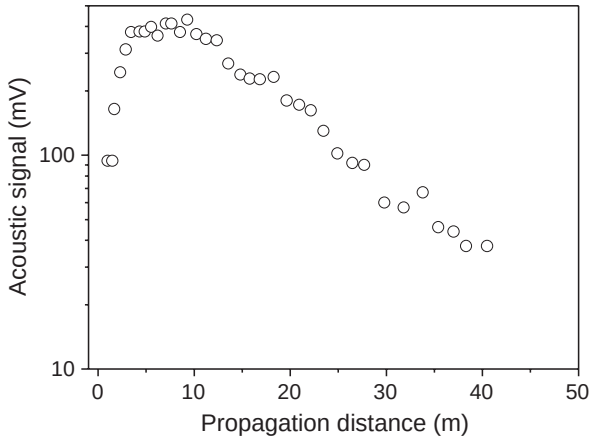

Fig. 4. Acoustic signal versus propagation distance for initially fully compressed pulses. Acoustic signal being proportional to the local peak free electron density is related to the light intensity in the filaments via the condition of equilibrium between Kerr focusing and plasma defocusing. Distance is measured relative to the output window of the container.

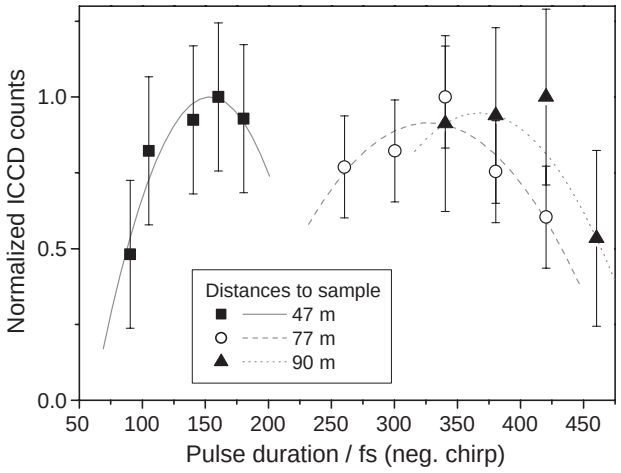

Fig. 5. Intensity of remotely detected copper line emission vs. negatively chirped pulse duration for three different sample distances. The maximums for different distances are arbitrarily normalized in order to plot experimental data in the same graph. Dashed parabolas are intended to guide the eye.

negative chirp leads to a longer filament starting distance. The following observations are common to optimum chirp settings at different distances: (a) onset of filamentation could be observed about 7 m before the sample, which corresponds well to what is indicated by the acoustic measurement (Fig. 4). Corresponding to this, (b) the filaments strong enough to ablate material from the sample were accompanied by bright white light spots on the sample, which are due to supercontinuum generated in the filaments before they hit the sample. (c) Ablating filaments could be identified by the clicking noise caused by shockwaves in consequence of ablations. Intense plasma line emission was expected when a high percentage of the filaments incident on the target were such strong ablating filaments.

The observed chirp dependence of LIBS signal can be explained by the dynamic nature of the process of multi-filamentation. During the life cycle of a filament, the peak intensity in its core can vary considerably, as shown by our acoustic measurement. Our experiments show that for a given sample distance, a suitable initial chirp allows a maximal plasma emission from the sample. They also confirm that the range of initial pulse durations which allows optimizing plasma emission becomes larger for a longer sample distance.

3.3. Filament-induced plasma emission as a function of sample distance

As discussed in the preceding paragraph, it is possible with an increasing negative chirp, to initiate filaments several meters before a sample is placed at an increasing distance. This procedure ensures a constant fluence contained in the filaments on a sample independently on its distance from the laser, provided that filaments are properly set to be initiated in the front of the sample. For a fixed detection system located nearby the laser, one expects a decrease of the detected signal due to geometrical factor $1/R^2$, where R denotes sample distance (or range of detection).

In Fig. 6 range-corrected plasma spectra from copper are shown for three different sample distances. These spectra

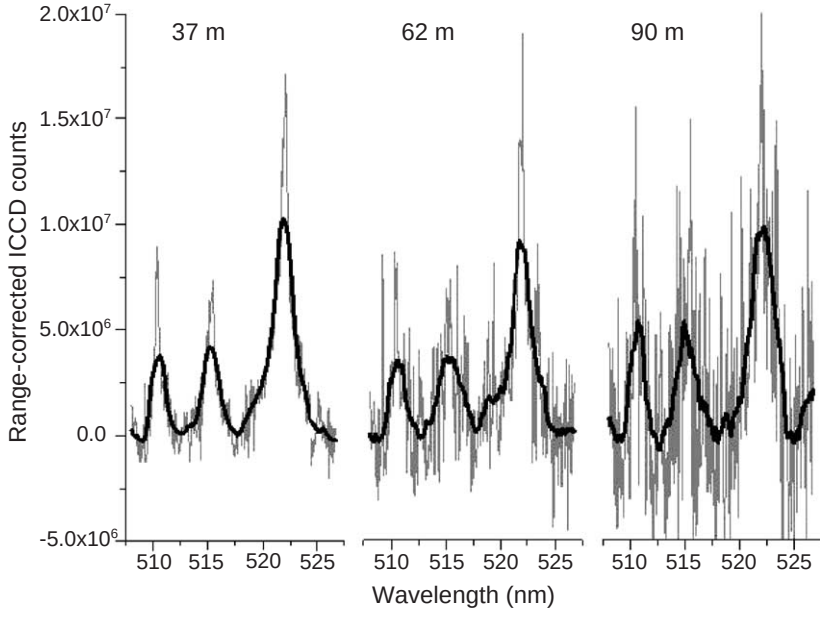

Fig. 6. Background- and range-corrected spectra of remotely detected copper plasma line emission (510.55 nm, 515.32 nm, and 521.82 nm) from three sample distances, 37 m, 62 m, and 90 m. Raw signals are plotted in grey. Thick black curves are obtained by smoothing raw spectra using an average of 32 adjacent points. All three spectra have been integrated over 1000 shots with an ICCD gate width of 10 μs. Despite the decrease of signal to noise ratio, the plot shows that there is no decrease of number of photons emitted by filament-induced plasma as sample distance increases.

have been acquired with an integration time of 100 s. Spectra have been multiplied by a factor of R^2 to compensate for the geometrical decrease. As it can be seen from the figure, range-corrected spectra have the same intensity for 37 m, 62 m and 90 m. This result demonstrates clearly that the number of initially emitted photons from the plasma is independent on the distance between laser and sample. This holds at least for a distance up to 90 m, which was limited by the available experimental space. Due to $1/R^2$ decrease of the number of collected photons, signal to noise ratio (SNR) decreases as sample distance increases. Assuming the number of photons emitted by plasma is the same at even longer distances, extrapolation of the spectra in Fig. 6 leads to an estimated maximal sample distance of 150 m for the used detection system, where the SNR reaches the value 1.

3.4. Filament-induced remote ablation at a distance of 180 m

In order to investigate the capability of filaments to generate plasma at distances exceeding the estimated limit of 150 m imposed by the used detection system, an aluminum sample was positioned at a distance of 180 m from the laser. Due to limitations inherent to the new target location (in an office at the fifth floor of a building), the second detection system was used to detect plasma emission near the sample.

The aluminum sample was irradiated by filaments. We optimized ablation by varying initial chirp. The supercontinuum generated in filaments by self-phase modulation being enough weak in the blue-UV region, plasma line emission from the aluminum sample at 394.4 nm and 396.1 nm could be detected without temporally gating the detection system. Elastic scattering of the supercontinuum from the sample was used to trigger a digital oscilloscope connected to the output of the PM. The wavelength transmitted by the spectrometer was scanned in steps of 1 nm in the region of the two strong atomic aluminum emission lines around 395 nm. The transient PM signals were averaged over 100 shots for each wavelength. Two representative transient signals are shown in Fig. 7, one corresponding to on-resonance setting of the spectrometer, and the second off-resonance spectrometer setting. The off-resonance curve represents elastically scattered supercontinuum. On the on-resonance curve, plasma line emission appears with a lifetime of about 130 ns. This decay time is much shorter than microsecond decay times that we observed with focused pulses (femtosecond, picosecond or nanosecond duration) at shorter distances [5].

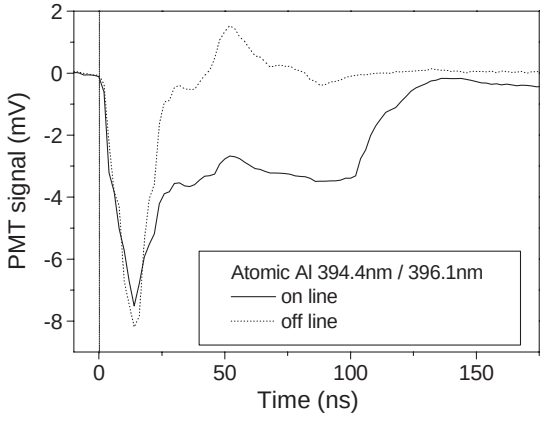

Fig. 7. Transient signals from filament-induced plasma emission from an aluminium target placed at 180 m from the laser. The on-line transient corresponds to the spectrometer tuned to one of aluminium lines. The off-line transient corresponds to the spectrometer tuned out of aluminium lines. The decay time of plasma emission can be estimated from the PM signal to be about 130 ns.

4. Discussion: towards the kilometer-range LIBS

Our results show that remote ablation can be induced by filaments at long distances. This opens the way to kilometer-range LIBS. In this section, we provide a parameter estimation for detection system required for the detection of plasma emission induced by filaments on a metallic sample placed at 1 km from the laser. Here we assume that filaments can be induced at distances of the order of 1 km, which is supported by experimental observations [17,35] and theoretical calculations [36].

The detection system used in present experiments (telescope, spectrometer, and ICCD camera) offers good spectral resolution and ease of use at the cost of low light throughput. The major bottlenecks are represented by the fiber bundle and the spectrometer itself. The fiber bundle unavoidably introduces Fresnel (reflection) losses and damping (transmission losses), which lead to a net transmittance of the fiber bundle of 55% around 520 nm (manufacturer data). Including the necessary *f*-number matching of the fiber output, light passing through the Czerny–Turner spectrometer suffers a total of five reflections from aluminum coated mirrors. Consequently, at wavelengths under consideration, the transmittance of the sequence of optical elements before the detector is at best 14%, including the spectral efficiency of the diffraction grating and assuming optimum coupling into the fiber bundle.

From the filament-induced plasma copper spectrum acquired from 90 m distance, one can estimate average number of photons originating from the copper 521.8 nm line and reaching the detector after each laser shot. This has been done by integrating the background-removed ICCD counts which can be attributed to this emission line, and by taking into account the spectral efficiency of the ICCD photocathode and the gain of the intensifier. Such estimation leads to an average of 19 photons reaching the detector at each laser shot. As it was mentioned before, such a small number of detected per-shot photons are due to the low transmittance of the used detection system.

For longer operation ranges, a dedicated detection system offering high light collection efficiency has to be designed.

Besides increasing the transmittance of the spectrometer, the aperture of the telescope has also to be increased. We propose an integrated combination of a Cassegrainian reflector telescope, a flat-field spectrograph and an ICCD detector. Compared to Newtonian design, folded Cassegrainian design offers compactness and a location of the focal plane situated behind the primary mirror, more convenient for attaching further instrumentation. A flat-field spectrograph has a flat-field imaging grating as its single optical element, which reduces the number of optical elements to a minimum and allows transmittance of the spectrometer to be practically given by grating reflectivity. A flat-field imaging grating is a holographically structured concave grating with modulated non-uniform line spacing allowing the spectrum to be imaged on a plane (i.e. the ICCD) instead on an arc on Rowland's circle. Such a design requires a telescope of far better imaging quality and pointing stability than the approach utilizing a fiber bundle.

High throughput is essentially achieved by reducing number of reflections, i.e. by keeping light path as direct as possible. However, that allows more direct paths for stray light as well. A challenge is to keep the rejection rate of stray light comparable to that of the present setup in order to finally improve the overall SNR. In this condition and assuming a realistic transmittance of 50% for the discussed telescope–spectrometer combination, the SNR can be increased from 1 to 3.57 (50:14%) for a sample distance of 150 m with the same ICCD detector as used in the present experiments. A larger primary mirror with diameter of 70 cm can be used to further increase the solid angle of the detection system by a factor of $(70/20)^2 = 12.25$. That would lead to a theoretical SNR of ~ 46 (12.25×3.57) for a sample distance of 150 m. It means that copper line emission from filament-generated plasma would be detectable with a SNR of 1 at a distance of ~ 1000 m ($150\ \mathrm{m} \times \sqrt{46}$) with an integration time comparable to that used in the present experiments.

Another approach to dramatically increase the sensitivity of the detection system with relatively small telescope (primary mirror diameter 40 cm for example) consists of the use of a single element detector such as a photomultiplier tube (PMT) coupled to a monochromator. This setup is actually similar to a LIDAR [37] detection with a well-known high sensitivity allowing an easy access to a multiple kilometer detection range. Our observation on transient plasma emission at a distance of 180 m from the laser demonstrates that due to low supercontinuum emission in the near UV range (especially interesting for LIBS), plasma emission can be detected by a PMT without any optical or electronic gating. Even though the low spectral resolution of PMT detection could limit analytical capability in this configuration, an elemental identification can be carried out with a compact detection system over a distance as far as filaments can propagate. In this case, the detection would not be the limiting factor for a long-range kilometer LIBS elemental identification.

5. Conclusion

We have demonstrated ablation of the surface of a metallic target placed at a distance up to 180 m using filaments induced by high intensity femtosecond pulses propagating in air. A quasi-periodical grating like ripple structure has been observed on the surface irradiated by filaments. Spatial period of the ripples is estimated to be 0.64 μm. Our observation provides the evidence of ripple structure on metallic sample induced by ultra-short laser pulses. The detection of plasma emission from the target corresponds to remote filament-induced breakdown spectroscopy, that we call R-FIBS. A remarkable property of a LIBS spectrum induced by femtosecond pulse is the absence of emission from ambient air, which is particularly interesting in case of analysis of a complex sample by the method of spectral correlation. For an increasing distance between the laser and the target, we have demonstrated that a properly increasing negative chirp leads to a constant plasma emission from the target, which means that for a detection system located nearby the laser system, LIBS signal only decreases as $1/R^2$, where R is the distance between the laser and the target. Finally, a parameter estimation based on our experimental data at 90 m shows that kilometer-range R-FIBS operation would be possible with an improved high-throughput spectrometer coupled to a telescope with a primary mirror of 70 cm diameter and an ICCD camera. Furthermore, a LIDAR type detection system including a monochromator and a PMT would allow a R-FIBS elemental identification over a very long distance, as far as filaments propagate in the atmosphere, with a detection system based on a compact telescope.

Acknowledgements

This work has been carried out within the framework of the Teramobile Project funded by Centre National de la Recerche Scientifique (CNRS), Deutsche Forschungsgemeinschaft (DFG), Ministère des Affaires Etrangères Français (MAE), Deutsche Akademische Austauschdienst (DAAD). The website of the Teramobile project is www.teramobile.org. We would like to thank Dr. R. Bourayou for his contribution in the acoustic measurement of longitudinal plasma profile in filaments. Kamil Stelmaszczyk would like to acknowledge the fellowship of Alexander von Humbold Foundation.

References

[1] Special issue on laser-induced breakdown spectroscopy, Spectrochim. Acta B 56 (2002).
[2] Special issue on laser-induced breakdown spectroscopy, J. Anal. At. Spectrom. 19 (2004).
[3] L.J. Radziemski, D.A. Cremers, Spectrochemical analysis using laser plasma excitation, in: L.J. Radziemski, D.A. Cremers (Eds.), Laser-

Induced Plasma: Physical, Chemical and Biological Applications, Marcel Dekker, New York, 1989.
[4] S. Michael Angel, Dimitra N. Stratis, Kristine L. Eland, Tianshu Lai, Mark A. Berg, David M. Gold, LIBS using dual- and ultra-short laser pulses, J. Anal. Chem. 369 (2001) 320–327.
[5] P. Rohwetter, K. Stelmaszczyk, G. Méjean, J. Yu, E. Salmon, J. Kasparian, J.P. Wolf, L. Wöste, Remote LIBS with ultrashort pulses: characteristics in picosecond and femtosecond regimes, J. Anal. At. Spectrom. 19 (2003) 437–444.
[6] Homeland security drives LIBS forward, Opto- and -Laser-Europe. 112 (Dec. 2003) 13–15.
[7] S. Hamilton, R. Al-Wazzan, A. Hanvey, A. Varagnat, S. Devlin, Fully integrated wide range LIBS system with high UV efficiency and resolution, J. Anal. At. Spectrom. 19 (2003) 479–482.
[8] Santiago Palanco, Simon Conesa, Javier Laserna, Pulse energy requirements for remote analysis with LIBS beyond the 100 meter range paper W3-2, 3rd International Conference, LIBS 2004, September 28–October 1 2004, Torremolinos (Malaga), Spain, 2004.
[9] K. Stelmaszczyk, P. Rohwetter, G. Méjean, J. Yu, E. Salmon, J. Kasparian, R. Ackermann, J.-P. Wolf, L. Wöste, Long-distance remote laser-induced breakdown using filamentation in air, Appl. Phys. Lett. 85 (2004) 3977–3979.
[10] J.H. Marburger, Self-focusing: theory, Prog. Quantum Electron 4 (1975) 35.
[11] A. Braun, G. Korn, X. Liu, D. Du, J. Squier, G. Mourou, Self-channeling of high-peak-power femtosecond laser pulses in air, Opt. Lett. 20 (1995) 73–75.
[12] A. Chiron, B. Lamouroux, R. Lange, J.F. Ripoche, M. Franco, B. Prade, G. Bonnaud, G. Riazuelo, A. Mysyrowicz, Numerical simulations of the nonlinear propagation of femtosecond optical pulses in gases, Eur. Phys. J. D 6 (1999) 383–396.
[13] J. Kasparian, R. Sauerbrey, S.L. Chin, The critical laser intensity of self-guided light filaments in air, Appl. Phys., B 71 (2000) 877–879.
[14] A. Becker, N. Aközbek, K. Vijayalakshmi, E. Oral, C.M. Bowden, S.L. Chin, Intensity clamping and re-focusing of intense femtosecond laser pulses in nitrogen molecular gas, Appl. Phys., B 73 (2001) 287–290.
[15] B. La Fontaine, F. Vidal, Z. Jiang, C.Y. Chien, D. Comtois, A. Desparois, T.W. Johnston, J.-C. Kieffer, H. Pépin, H.P. Mercure, Filamentation of ultrashort pulse laser beam resulting from their propagation over long distance in air, Phys. Plasmas 6 (1999) 1615–1621.
[16] H. Wille, M. Rodriguez, J. Kasparian, D. Mondelain, J. Yu, A. Mysyrowicz, R. Sauerbrey, J.P. Wolf, L. Wöste, Teramobile: a mobile femtosecond–terawatt laser and detection system, Eur. Phys. J., Appl. Phys. 20 (2002) 183–190.
[17] M. Rodriguez, R. Bourayou, G. Méjean, J. Kasparian, J. Yu, E. Salmon, A. Scholz, B. Stecklum, J. Eislöffel, U. Laux, P. Hatzes, R. Sauerbrey, L. Wöste, J.-P. Wolf, Kilometer-range non-linear propagation of fs laser pulses, Phys. Rev., E 69 (2004) 036607.
[18] J. Kasparian, M. Rodriguez, G. Méjean, J. Yu, E. Salmon, H. Wille, R. Bourayou, S. Frey, Y.B. Andre, A. Mysyrowicz, R. Sauerbrey, J.P. Wolf, L. Woeste, White light filaments for atmospheric analysis, Science 301 (2003) 61–64.
[19] D. Strickl, G. Mourou, Compression of amplified chirped pulses, Opt. Commun. 56 (1985) 219.
[20] S. Skupin, L. Bergé, U. Peschel, F. Lederer, G. Méjean, J. Yu, J. Kasparian, E. Salmon, J.-P. Wolf, M. Rodriguez, L. Wöste, R. Bourayou, R. Sauerbrey, Filamentation of femtosecond light pulses in the air: turbulent cells versus long-range clusters, Phys. Rev., E 70 (2004) 046602.
[21] M. Mlejnek, E.M. Wright, J.V. Moloney, Power dependence of dynamic spatial replenishment of femtosecond pulses propagating in air, Opt. Express 4 (1999) 223–228.
[22] N. Aközbek, M. Scalora, C.M. Bowden, S.L. Chin, White-light continuum generation and filamentation during the propagation of ultra-short laser pulses in air, Opt. Commun. 191 (2001) 353–362.
[23] Jeff F. Young, J.S. Preston, H.M. van Driel, J.E. Sipe, Laser-induced periodic surface structure: II. Experiments on Ge, Si, Al, and brass, Phys. Rev., B 27 (1983) 1155–1172.
[24] J.E. Sipe, J.F. Young, J.S. Preston, H.M. van Driel, Laser-induced periodic surface structure: I. Theory, Phys. Rev., B 27 (1983) 1141–1153.
[25] F. Costache, M. Henyk, J. Reif, Modification of dielectric surface with ultra-short laser, Appl. Surf. Sci. 186 (2002) 352–357.
[26] J. Reif, F. Costache, M. Henyk, S.V. Pandelov, Ripple revisited: non-classical morphology at the bottom of femtosecond laser ablation craters in transparent dielectrics, Appl. Surf. Sci. 197–198 (2002) 891–895.
[27] F. Costache, M. Henyk, J. Reif, Surface patterning on insulators upon femtosecond laser ablation, Appl. Surf. Sci. 208–209 (2003) 486–491.
[28] H.O. Jeschke, M.E. Garcia, K.H. Bennemann, Theory for the ultrafast ablation of graphite film, Phys. Rev. Lett. 87 (2001) 015003.
[29] H.O. Jeschke, M.E. Garcia, K.H. Bennemann, Time-dependent energy absorption changes during ultrafast lattice deformation, J. Appl. Phys. 91 (2002) 18–23.
[30] A. Gomes, A. Aubreton, J.J. Gonzalez, S. Vacquié, Experimental and theoretical study of the expansion of a metallic vapour plasma produced by laser, J. Phys. D: Appl. Phys. 37 (2004) 669–689.
[31] Samuel S. Mao, Xianglei Mao, Ralph Greif, Richard E. Russo, Initiation of an early-stage plasma during picosecond laser ablation of solids, Appl. Phys. Lett. 77 (2000) 2464–2466.
[32] Alan C. Samuels, Frank C. DeLucia Jr., Kevin L. McNesby, Andrzej W. Miziolek, Laser-induced breakdown spectroscopy of bacterial spores, molds, pollens, and protein: initial studies of discrimination potential, Appl. Opt. 42 (2003) 6205–6209.
[33] J. Yu, D. Mondelain, J. Kasparian, E. Salmon, S. Geffroy, C. Favre, V. Boutou, J.P. Wolf, Sonographic probing of laser filaments in air, Appl. Opt. 42 (2003) 7117–7120.
[34] S.A. Hosseini, J. Yu, Q. Luo, S.L. Chin, Multi-parameter characterization of the longitudinal plasma profile of a filament: a comparative study, Appl. Phys., B 97 (2004) 519–523.
[35] G. Méchain, A. Couairon, Y.B. André, C. D'Amico, M. Franco, B. Prade, S. Tzortzakis, A. Mysyrowicz, R. Sauerbrey, Long-range self-channeling of infrared laser pulses in air: a new propagation regime without ionization, Appl. Phys., B 79 (2004) 379–382.
[36] P. Sprangle, J.R. Peñano, B. Hafizi, Propagation of intense ultrashort pulses in the atmosphere, Phys. Rev., E 66 (2002) 046418.
[37] Raymond M. Measures, Laser Remote Sensing, Wiley, New York, 1992.